

Multiple antisense oligonucleotides targeted against monoacylglycerol acyltransferase 1 (*Mogat1*) improve glucose metabolism independently of *Mogat1*



Andrew J. Lutkewitte¹, Jason M. Singer¹, Trevor M. Shew¹, Michael R. Martino¹, Angela M. Hall¹, Mai He², Brian N. Finck^{1,*}

ABSTRACT

Objective: Monoacylglycerol acyltransferase (MGAT) enzymes catalyze the synthesis of diacylglycerol from monoacylglycerol. Previous work has suggested the importance of MGAT activity in the development of obesity-related hepatic insulin resistance. Indeed, antisense oligonucleotide (ASO)-mediated knockdown of *Mogat1* mRNA, which encodes MGAT1, reduced hepatic MGAT activity and improved glucose tolerance and insulin resistance in high-fat diet (HFD)-fed mice. However, recent work has suggested that some ASOs may have off-target effects on body weight and metabolic parameters via activation of the interferon alpha/beta receptor 1 (IFNAR-1) pathway.

Methods: Mice with whole-body *Mogat1* knockout or a floxed allele for *Mogat1* to allow for liver-specific *Mogat1*-knockout (by either a liver-specific transgenic or adeno-associated virus-driven Cre recombinase) were generated. These mice were placed on an HFD, and glucose metabolism and insulin sensitivity were assessed after 16 weeks on diet. In some experiments, mice were treated with control scramble or *Mogat1* ASOs in the presence or absence of IFNAR-1 neutralizing antibody.

Results: Genetic deletion of hepatic *Mogat1*, either acutely or chronically, did not improve hepatic steatosis, glucose tolerance, or insulin sensitivity in HFD-fed mice. Furthermore, constitutive *Mogat1* knockout in all tissues actually exacerbated HFD-induced obesity, insulin sensitivity, and glucose intolerance on an HFD. Despite markedly reduced *Mogat1* expression, liver MGAT activity was unaffected in all knockout mouse models. *Mogat1* overexpression in hepatocytes increased liver MGAT activity and TAG content in low-fat-fed mice but did not cause insulin resistance. Multiple *Mogat1* ASO sequences improved glucose tolerance in both wild-type and *Mogat1* null mice, suggesting an off-target effect. Hepatic IFNAR-1 signaling was activated by multiple *Mogat1* ASOs, but its blockade did not prevent the effects of either *Mogat1* ASO on glucose homeostasis.

Conclusion: These results indicate that genetic loss of *Mogat1* does not affect hepatic MGAT activity or metabolic homeostasis on HFD and show that multiple *Mogat1* ASOs improve glucose metabolism through effects independent of targeting *Mogat1* or activation of IFNAR-1 signaling.

© 2021 The Authors. Published by Elsevier GmbH. This is an open access article under the CC BY-NC-ND license (<http://creativecommons.org/licenses/by-nc-nd/4.0/>).

Keywords Monoacylglycerol acyltransferase; Insulin resistance; Antisense oligonucleotides; Interferon alpha/beta receptor 1

1. INTRODUCTION

Nonalcoholic fatty liver disease (NAFLD) results from ectopic hepatic lipid accumulation (steatosis) and is believed to be a key driver of many metabolic abnormalities associated with obesity, including insulin resistance and diabetes [1,2]. In obesity, the liver is overloaded with fatty acids from dietary intake, increased adipose tissue lipolysis, and higher rates of *de novo* lipid synthesis [3–5]. The liver must efficiently store these lipids as neutral triacylglycerol (TAG) to prevent deleterious effects of toxic lipid intermediates, such as activation of inflammation, endoplasmic reticulum (ER) stress, and insulin resistance [6].

There are two pathways of TAG synthesis in the liver: the glycerol-3-phosphate (G-3-P) pathway and the monoacylglycerol O-acyltransferase (MGAT) pathway. These pathways converge at diacylglycerol (DAG); the sole precursor of TAG [7–9]. MGATs acylate monoacylglycerol to form DAG and this enzymatic activity is encoded by several genes including *Mogat1*, *Mogat2*, and *Dgat1* in mice [10–13]. The importance of MGAT activity in intestinal absorption of dietary fat has long been studied [8,14]. Generally, the G-3-P pathway is considered to be the primary route of TAG synthesis in tissues other than the intestine, and the MGAT pathway is believed to be an auxiliary pathway. We have recently demonstrated that *Mogat1* is highly expressed in adipocytes and may function to suppress aberrant

¹Department of Medicine, Washington University School of Medicine, St. Louis, MO, United States ²Department of Pathology and Immunology, Washington University School of Medicine, St. Louis, MO, United States

*Corresponding author. Center for Human Nutrition, Washington University School of Medicine, 660 Euclid Ave., Box 8031, St. Louis, MO, 63110, United States. E-mail: bfinck@wustl.edu (B.N. Finck).

Received January 26, 2021 • Revision received February 17, 2021 • Accepted March 1, 2021 • Available online 3 March 2021

<https://doi.org/10.1016/j.molmet.2021.101204>

lipolysis [15]. In addition, the expression and activity of the MGATs are increased in humans and mouse models of NAFLD [16–20]. Suppression of hepatic and adipose tissue *Mogat1* expression, through use of antisense oligonucleotides (ASO), reduces hepatic MGAT activity and improves hepatic insulin sensitivity and glucose metabolism without affecting hepatic DAG or TAG levels in obese mice [17,18].

Second-generation ASOs are known to target multiple tissues, including liver, adipose, and intestine, all of which have MGAT activity [21]. Moreover, off-target effects of ASO treatment have also been described [22]. McCabe et al. recently demonstrated weight loss, adipocyte browning, and improvement in adipose tissue metabolism by ASO treatment that was independent of target gene knockdown [22]. These effects were mediated through the activation of interferon alpha/beta receptor 1 (IFNAR-1) signaling in adipose-derived macrophages [22]. Thus, we sought to obtain rigorous and independent confirmation that hepatic *Mogat1* plays an important role obesity-related hepatic insulin resistance and metabolic abnormalities using novel liver-specific and global *Mogat1* knockout mice. Our data surprisingly suggest that multiple *Mogat1* ASO sequences improve glucose metabolism through MGAT1-independent mechanisms and that the effects are not mediated through IFNAR-1 activation.

2. METHODS

2.1. Generation of mouse models

All mouse studies were approved by the Institutional Animal Care and Use Committee of Washington University. Due to the resistance of female mice to the effects of high fat diet (HFD), male mice in the C57BL6/J background were used in all studies. Mice were group housed and maintained on standard laboratory chow on a 12 h light/dark cycle. At eight-weeks of age mice were placed on control low-fat diet (LFD, Research Diets, 10 kcal, % fat matched sucrose, D12450J) or HFD (Research Diets, 60 kcal % fat, D12492) for the durations indicated. ASO treatments were performed as previously described [17]. Briefly, starting at 16 weeks on diet, mice were given twice weekly intraperitoneal injections of ASO directed against *Mogat1* (sequence #1: 5'-GATCTTGGCCACGTGGAGAT-3' (20-mer), or sequence #2: 5'-TGGCCACGTGGAGATACGAT-3' (20-mer), where indicated) or scramble control (Ionis, Pharmaceuticals, Inc., Carlsbad, CA; 25 mg/kg body weight) for three weeks.

Embryonic stem (ES) cells used to generate *Mogat1* whole-body knockout and *Mogat1* floxed mice were obtained from the Knockout Mouse Consortium (KOMP, project# CSD35789) [15]. Briefly, these ES cells contained a *Mogat1* allele wherein a cassette containing cDNAs encoding LacZ and a neomycin-resistance locus was inserted just upstream of *Mogat1* exon 4 that was flanked by LoxP sites. *Mogat1* exon 4 encodes the HPHG catalytic site of MGAT1, and thus loss of this exon will result in loss of its enzymatic activity. Resulting chimeric offspring from ES cell injections were mated to C57BL6/J mice to establish a line of constitutive whole-body *Mogat1* knockout mice. Other heterozygous whole-body knockout mice were crossed to transgenic mice expressing Flp recombinase to remove the LacZ/Neo cassette and generate the *Mogat1* floxed line. These mice were then crossed with mice expressing albumin promoter-driven Cre recombinase (Jackson Laboratory, B6.Cg-Speer6-ps1Tg (Alb-cre)21Mgn/J). Control mice are considered *Mogat1* floxed mice without the expression of the albumin promoter-driven Cre recombinase.

Acute liver-specific knockout mice were generated by retro-orbital injection of *Mogat1* floxed mice with 2.0×10^{11} genomic copies (GC) of adeno-associated virus serotype 8 (AAV8) expressing Cre recombinase under the control of human thyroid hormone-binding

globulin (TBG) promoter (Vector Biolabs, VB1724). Control mice received AAV8 expressing enhanced green fluorescent protein (eGFP) under control of the same promoter (Vector Biolabs, VB1743). For hepatic *Mogat1* overexpression, eight-week-old male C57BL6/J mice were given LFD or HFD for six weeks, then administered AAV8-TBG-eGFP or AAV8-TBG-mouse-*Mogat1* by retro-orbital injection (Vector Biolabs, VB1743, custom refseq# BC106135) and continued on diet for the times indicated.

In the IFNAR-1 inhibition study, HFD-fed male C57BL/6J mice were obtained from Jackson Laboratory after 12 weeks of HFD feeding. After acclimation and four additional weeks of HFD feeding, mice were weight matched into four treatment groups. Mice were given scramble ASO or ASOs targeting *Mogat1* as described above. During each ASO treatment, mice were also given intraperitoneal (IP) injections of IgG control (BioCell *InVivoMAB*, #BE0083, clone MOPC-21) or a monoclonal neutralizing antibody targeting interferon alpha/beta receptor 1 (IFNAR-1) (BioCell *InVivoMAB*, #BE0241, clone MAR1-5A3) [23]. Antibody treatments were given as IP injections of 250 ug per mouse in 100 uL of dilution buffer (BioCell, *InVivoPure* Ph 6.5 Dilution Buffer, #IP0065) twice a week for the first two weeks of ASO treatment, followed by three separate injections of 500 ug per mouse the third week of ASO treatments.

Prior to sacrifice, mice were fasted for 4 h starting at 0900. Mice were euthanized via CO₂ asphyxiation. Blood was collected from venipuncture of the inferior vena cava into EDTA-coated tubes, and plasma was removed by centrifugation. Liver and other tissues were immediately collected, flash-frozen in liquid nitrogen, and stored at -80 °C until further use.

2.2. Histology and NAFLD scoring

Liver tissue was harvested as described in section 2.1. Immediately following dissection, livers were fixed in 10% buffered formalin for 48 h. Liver tissue was rinsed and stored in 70% EtOH until paraffin embedding, sectioning, and staining with hematoxylin-eosin (H&E) in the Anatomic and Molecular Pathology Core Labs at Washington University School of Medicine. H&E sections were used to determine NAFLD activity score by a blinded independent clinical pathologist [24].

2.3. Metabolic phenotyping of mouse models

Glucose tolerance tests (GTTs) were performed in mice fasted for 5 h starting at 0900. Mice were given an IP injection of glucose (1 g/kg body weight dissolved in saline), and blood glucose was measured from the tail using a One Touch Ultra glucometer (Life Scan, Inc.) at the times indicated. For insulin tolerance tests (ITTs), mice were fasted for 4 h before IP injections of recombinant Humulin R® (0.75 U/kg body weight in saline). Tolerance tests were performed one week apart to allow the mice to recover starting at 15 and 16 weeks of diet or week two and three of acute treatments. Body composition was determined in fed mice using ECHO MRI. Because the whole-body null mice had differences in body weights compared to WT mice, the tolerance tests in these mice were dosed based on lean mass (1 g glucose/kg lean mass and 1.5 U insulin/kg lean mass).

2.4. Liver lipids and plasma metabolites

Frozen liver pieces were homogenized with bead disruption in phosphate-buffered saline (PBS, 100 mg/mL). Lipids were solubilized in 1% sodium deoxycholate via vortexing and heating at 37 °C for 5 min. Triglycerides and total cholesterol were measured enzymatically using the Infinity triglyceride and cholesterol colorimetric assay kits (Thermo Fisher, TR22421 and TR13421) and normalized to mg tissue (wet weight). Plasma insulin was determined by Singulex

Immunoassay (Millipore Sigma) via the Washington University Core Laboratory for Clinical Studies. Plasma ALT and AST were measured using TECO Diagnostic liquid kinetic assays (A524 and A559).

2.5. mRNA isolation and quantitative polymerase chain reaction (PCR)

Total liver RNA was isolated from frozen liver samples using RNA STAT (Iso Tech, CS-502) according to the manufacturer's protocol. RNA was reverse transcribed into cDNA using Taqman high-capacity reverse transcriptase (Life Technologies, 43038228). Quantitative PCR was performed using Power SYBR green (Applied Biosystems, 4367659) and measured on an ABI PRISM 7500 or ABI QuantStudio 3 sequence detection system (Applied Biosystems). Results were quantified using the $2^{-\Delta\Delta Ct}$ method and shown as arbitrary units relative to control groups. Primer sequences are listed in [Supplemental Table 1](#).

2.6. Primary hepatocyte isolations

Primary hepatocytes were isolated as previously described [25]. Briefly, 10- to 16-week-old female mice were given an overdose of isoflurane prior to perfusions. The livers were perfused via catheterization of the hepatic portal vein and flushed with 30 mL of HBSS (Ca^{2+}/Mg^{2+} -free, 0.5 mM EGTA) prior to digestion with 20 mL of collagenase solution Type IV collagenase (sigma S5138) at 1 mg/mL in DMEM (serum free, 1 mM sodium pyruvate). Following perfusion, the livers were removed and disrupted in the collagenase solution. Cells were added to ice-cold complete DMEM (10% FBS, 1 mM sodium pyruvate, 100 U PenStrep, 0.25 μ g/mL amphotericin b) and passed through a 50- μ m filter prior to centrifugation at 50g \times 2 min. The supernatant was removed, and hepatocytes were resuspended in complete DMEM and washed two more times. Five hundred thousand cells were then directly added to RNA STAT for RNA isolation and quantification.

2.7. MGAT enzymatic assay

MGAT activity was determined as previously described [26]. Liver tissue (50 mg/mL) was homogenized by probe sonicated in ice-cold membrane buffer (50 mM Tris-HCl pH 7.4, 1 mM EDTA, 250 mM sucrose, and complete protease inhibitors table (Roche Diagnostics, A32965)). Homogenates were clear of whole-cell debris by low-speed centrifugation at 500g \times 10 min at 4 °C. The resulting supernatants were spun at 100,000 g \times 60 min at 4 °C using a Beckman benchtop ultra-centrifuge. The cytosolic fractions (supernatant) were removed, and the membranes were reconstituted via pipetting in membrane buffer without protease inhibitors. Proteins were quantified using the bicinchoninic acid (BCA) assay according to the manufacturer's protocols (Thermo Fisher, 23225). Fifty micrograms of membrane were incubated in assay buffer (5 mM MgCl₂, 1.25 mg/mL BSA, 200 mM sucrose, 100 mM Tris-HCl (pH 7.4)) containing 20 μ M of [¹⁴C]oleoyl-CoA (American Radiolabeled Chemicals, ARC 0527), and 200 μ M of sn-2-oleoylglycerol (Caymen Chemical, 16537) for 10 min. The reaction was stopped with 50 μ L of 1% phosphoric acid. Lipids were extracted in 2:1 v/v % CHCl₃:MeOH and separated by thin-layer chromatography in hexane/ethyl ether/acetic acid (80:20:1, v/v/v %). Samples were run against standards for oleic acid, 1, 3 diacylglycerol, and triglyceride, and corresponding spots were scraped from the plate and ¹⁴C-radioactivity was measured via scintillation counter. Backgrounds were calculated from reaction mixtures without membrane fractions.

2.8. Statistical analysis

Data were analyzed using GraphPad Prism software. Independent and paired T-tests, one-way analysis of variance (ANOVA), or factorial

ANOVAs were performed where appropriate. Secondary post-hoc analysis found differences in groups using either Tukey or Sidak multiple comparisons where appropriate. $P < 0.05$ was considered significant.

3. RESULTS

3.1. Liver-specific knockout of *Mogat1*

We generated mice with hepatocyte-specific deletion of *Mogat1*, and the resulting offspring were outwardly normal on a standard chow diet. When given *ad libitum* access to a 10% fat (low-fat diet, LFD) or 60% fat (HFD), the mice gained weight similar to littermate fl/fl controls ([Figure 1A](#)). Contrary to our previous studies showing a beneficial effect of *Mogat1* ASOs on metabolic parameters in obese mice, glucose and insulin tolerance was not different between genotypes on LFD or HFD ([Figure 1B,C](#)). We confirmed that *Mogat1* expression was markedly suppressed in *Mogat1* fl/fl Alb-Cre + livers and freshly isolated primary hepatocytes (of note, *Mogat1* expression drastically decreases after hepatocyte isolation and plating, data not shown) ([Figure 1D,E](#)). Hepatic TAG content increased with HFD but was similar between genotypes ([Figure 1F](#)). In contrast to previous work with *Mogat1* ASO-treated mice, MGAT activity in isolated liver membranes was not affected by *Mogat1* knockout ([Figure 1G](#) and ref. [17]). Therefore, gene expression of similar acyltransferases with known MGAT activity (*Mogat2*, *Dgat1*) and DGAT activity (*Dgat2*) were measured. *Mogat2* was not significantly increased in knockout mice, while both *Dgats* increased with HFD but were unaffected by *Mogat1* knockout ([Figure 1H](#)).

3.2. AAV8-mediated liver-specific knockout of *Mogat1*

To avoid possible compensation from chronic *Mogat1* knockout, we injected *Mogat1* fl/fl mice with an AAV8-TBG-Cre or eGFP control after 16 weeks of HFD feeding and assessed glucose homeostasis three weeks later ([Figure 2](#)). This paradigm was selected because three weeks of *Mogat1* ASO treatment after 16 weeks on diet is effective at improving insulin sensitivity and glucose homeostasis [16,17]. After three weeks, compared to GFP controls, AAV8-Cre knockout mice had similar body weight and no differences in glucose or insulin tolerance ([Figure 2A–C](#)). The AAV8-Cre reduced *Mogat1* expression ([Figure 2D](#)). Similar to constitutive *Mogat1* liver-specific knockout, acute deletion of hepatic *Mogat1* did not alter liver TAG content and slightly increased MGAT activity ([Figure 2E,F](#)). Gene expression of similar acyltransferases (*Mogat2*, *Dgat1*, *Dgat2*) were unaffected by *Mogat1* knockout ([Figure 2G](#)) [10–13]. These data indicate that genetic deletion of *Mogat1* in the livers of diet-induced obese mice for 3 weeks does not affect glucose or insulin tolerance, and may suggest compensation from other enzymes with MGAT activity [11,12,27].

3.3. *Mogat1* whole-body deletion

Mogat1 ASO treatment likely results in gene knockdown in multiple tissues [18,21]. Thus, we generated *Mogat1* whole-body null mice (MOKO) to delete *Mogat1* in all tissues ([Figure 3](#)). MOKO mice were outwardly normal on standard chow diet. Unexpectedly, when given an HFD, MOKO mice gained more total body weight than littermate wild-type (WT) control mice ([Figure 3A,B](#)). The heterozygous littermates had an intermediate phenotype (data not shown). The increase in weight gain was not attributed to increased adiposity as evidenced by fat mass and percent adiposity in ECHO MRI and individual fat pad weights and thus may be due to larger body size ([Figure 3B](#) and [Supplemental Fig. 1](#)). Glucose tolerance was not affected by *Mogat1* knockout ([Figure 3C](#)). However, HFD-fed MOKO mice had reduced insulin

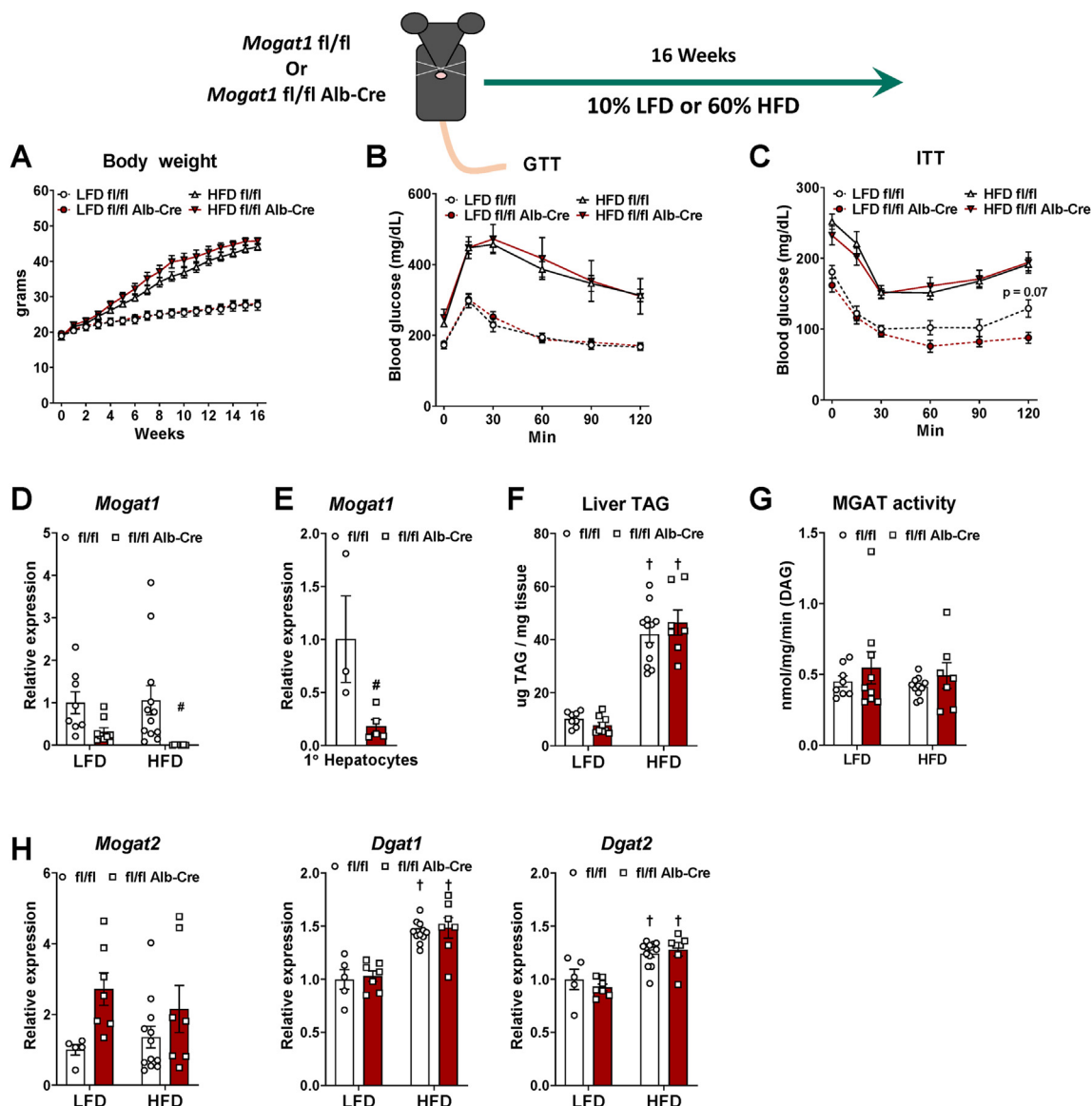


Figure 1: Constitutive liver-specific *Mogat1* deletion does not improve insulin sensitivity in mice. Male *Mogat1* fl/fl mice and littermate *Mogat1* fl/fl albumin Cre + mice were fed an LFD or an HFD starting at 8 weeks of age for 16 weeks. Mice were fasted for 4 h prior to sacrifice and tissue collection. A: HFD increased body weight in both groups. B,C: HFD-fed mice have impaired glucose and insulin tolerance compared to LFD groups. D,E: *Mogat1* gene expression is reduced in knockout liver and primary hepatocytes. F: HFD increased liver TAG content in both genotypes. G: MGAT activity was not affected by diet or genotype. H: Gene expression of *Mogat2*, *Dgat1*, and *Dgat2* were unaffected by *Mogat1* knockout. Data are expressed as means \pm S.E.M, and significance was assessed by two-way ANOVA with Sidak's multiple comparison test, # $p < 0.05$ gene effect, and † $p < 0.05$ diet effect; $n = 5-10$ for mouse studies. $n = 3-5$ female mice for primary hepatocyte isolations and two-tailed Student's t-test were performed, # $p < 0.05$ gene effect.

tolerance and increased plasma insulin concentrations, which could be indicative of insulin resistance (Figure 3D,E). *Mogat1* gene expression was undetectable in livers of MOKO mice (Figure 3F) or in any other tissue analyzed (data not shown). MOKO mice had similar TAG content and MGAT activity (Figure 3G,H). Similar to the liver-specific knockout models, MOKO mice had no increases in hepatic *Mogat2*, *Dgat1*, and *Dgat2* (Figure 3J).

3.4. Hepatic *Mogat1* overexpression

We next aimed to determine whether overexpression of hepatic *Mogat1* was sufficient to promote hepatic steatosis, insulin resistance, and deleterious effects on systemic glucose metabolism. We fed C57BL/6J mice an LFD for six weeks then injected them with AAV8 expressing

either *GFP* or mouse *Mogat1* under control of the hepatocyte-specific TBG promoter and continued them on diet for an additional ten weeks (Figure 4). *Mogat1* overexpressing (OE) mice gained similar weight as the GFP control-treated mice (Figure 4A). After 16 weeks (ten weeks of overexpression), there was no difference in glucose or insulin tolerance between groups (Figure 4B,C). *Mogat1* gene expression was significantly increased by the administration of the AAV8-*Mogat1* (Figure 4D). MGAT1 overexpression increases liver TAG and MGAT activity (Figure 4E,F). Despite the increases in MGAT activity and hepatic TAG content, *Mogat1* overexpression did not alter liver histology or markers of NAFLD progression, including liver cholesterol, NAFLD score, or plasma alanine aminotransferase (ALT) and aspartate aminotransferase (AST) (Figure 4G and Supplemental Fig. 2).

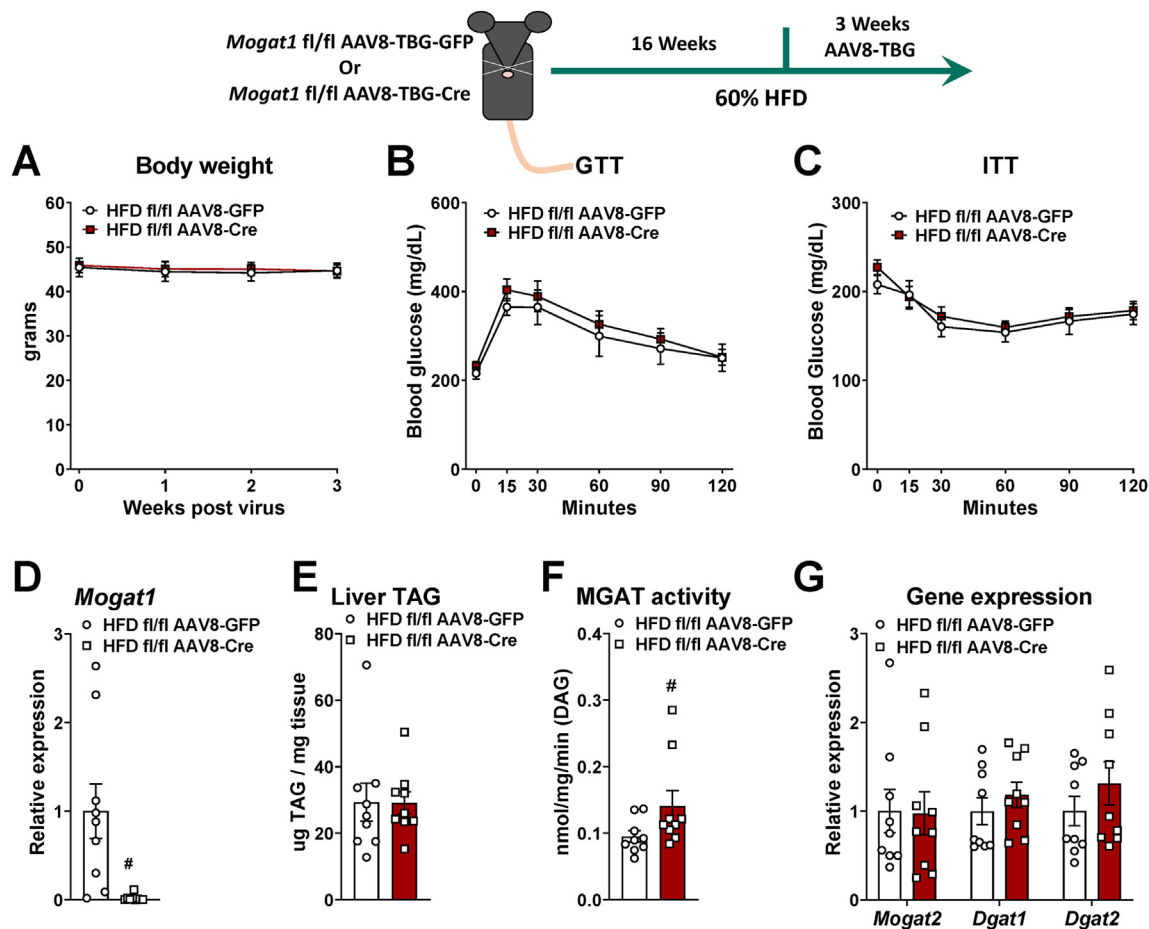


Figure 2: Acute liver-specific deletion of *Mogat1* does not improve glucose or insulin tolerance in HFD-fed mice. Male *Mogat1* fl/fl mice were fed an HFD starting at 8 weeks of age. After 16 weeks, mice were given a retro-orbital injection of AAV8-TBG-GFP or Cre recombinase (2×10^{11} GC per mouse) and remained on diet for an additional 3 weeks. Mice were fasted for 4 h prior to sacrifice and tissue collection. A: Acute liver-specific *Mogat1* knockout did not affect body weight. B,C: *Mogat1* knockout did not improve glucose or insulin tolerance. D: *Mogat1* knockout reduced *Mogat1* gene expression in liver. E: Liver TAG content was not different among groups. G: Hepatic MGAT activity was increased by acute *Mogat1* knockdown in liver. *Mogat1* knockout did not increase *Mogat2*, *Dgat1*, or *Dgat2* gene expression in liver. Data are expressed as means \pm S.E.M., and two-tailed Student's *t*-tests were performed, #*p* < 0.05 gene effect, *n* = 9.

Utilizing the same overexpression regimen, we investigated whether *Mogat1* overexpression exacerbates hepatic steatosis and insulin resistance during HFD feeding (Figure 5). Similar to the LFD-fed mice, *Mogat1* overexpression did not affect body weight or glucose and insulin tolerance in HFD-fed mice (Figure 5A–C). *Mogat1* gene expression was significantly increased by the AAV8-*Mogat1*-OE treatment (Figure 5D). Unlike the LFD-fed mice, hepatic TAG and MGAT activity were not different between groups (Figure 5E,F). Similarly, *Mogat1* overexpression did not alter liver histology or markers of NAFLD progression in HFD-fed mice (Figure 5G and Supplemental Fig. 2). Thus, we concluded that hepatic *Mogat1* overexpression is sufficient to increase hepatic triglyceride accumulation on an LFD, but not insulin resistance or systemic dysregulation of glucose metabolism.

3.5. *Mogat1* ASO treatment improves hepatic insulin sensitivity on HFD

To confirm our previous reports indicating that *Mogat1* suppression by ASO improves hepatic insulin sensitivity [17,18], we fed C57BL6/J mice with an HFD. After 16 weeks, mice were weight-matched and randomized to receive ASOs targeting either *Mogat1* or scramble

control (Figure 6). As previously described [17], *Mogat1* ASO treatment did not affect body weight but reduced blood glucose and plasma insulin levels on an HFD (Figure 6A–C). *Mogat1* and *Mogat2* expression was increased by the HFD and *Mogat1* ASO treatments suppressed *Mogat1* without affecting *Mogat2* (Figure 6D,E). MGAT activity was reduced without affecting liver TAG content (Figure 6F,G). Moreover, glucose tolerance was improved in mice using two different *Mogat1* targeting ASO sequences in HFD fed mice (Supplemental Fig. 3). Together, these data confirm our previous reports that multiple *Mogat1* ASO sequences improve hepatic metabolism during an HFD challenge.

3.6. *Mogat1* ASO treatment improves glucose tolerance in *Mogat1* whole-body null mice

Given the inability to reproduce the insulin-sensitizing effects of *Mogat1* ASOs in any of our genetic models, we tested whether *Mogat1* ASO treatment improves glucose metabolism independent of *Mogat1*. We treated MOKO mice, fed an HFD for 16 weeks, with multiple ASOs targeting *Mogat1* or scramble control (Figure 7 and Supplemental Fig. 4). Remarkably, *Mogat1* ASO treatment improved glucose tolerance in both MOKO and WT mice as indicated by the area under the

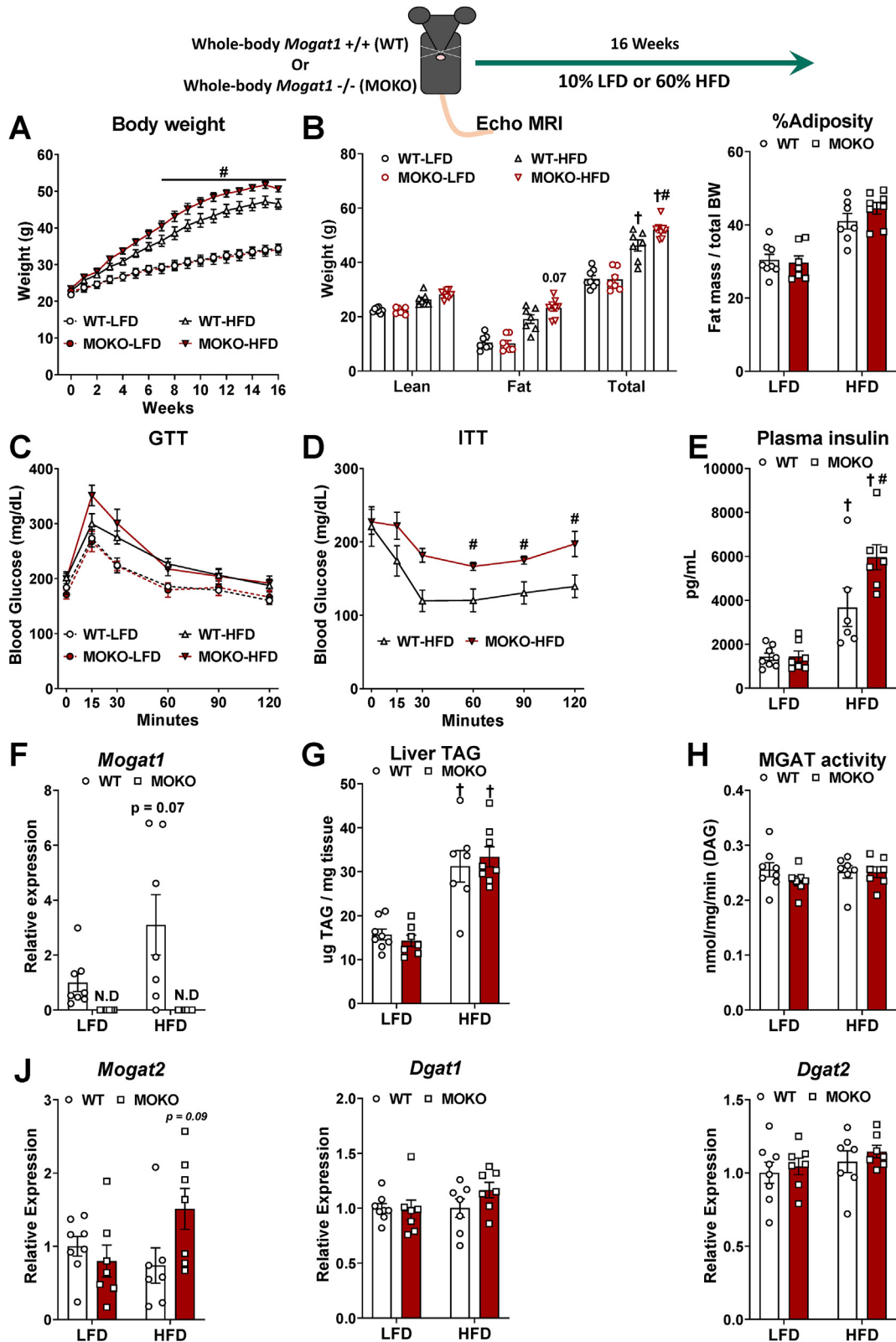


Figure 3: Whole-body deletion of *Mogat1* causes weight gain and insulin intolerance on an HFD. Male wild-type (WT) and littermate *Mogat1* whole-body knockout (MOKO) mice were fed an LFD or an HFD starting at 8 weeks of age for 16 weeks. Mice were fasted for 4 h prior to sacrifice and tissue collection. A: *Mogat1* knockout mice gain (MOKO) more weight on an HFD than littermate WT controls. B: ECHO MRI indicates MOKO mice have increased whole body mass, while compared to WT controls. C: Glucose tolerance (1 g/kg lean mass) was not significantly changed in MOKO mice. D,E: HFD-fed MOKO mice had significantly impaired insulin tolerance (1.5 U/kg lean mass) and plasma insulin levels compared to WT controls. F: *Mogat1* gene expression was not detectable in MOKO mice on either diet. G: Liver TAG was increased by HFD but unaffected by genotype. H: MGAT activity was unaffected by either diet or genotype. Data are expressed as means \pm S.E.M, and two-way ANOVA with Sidak's or Tukey's multiple comparison tests were performed where appropriate, # $p < 0.05$ gene effect, † $p < 0.05$ diet effect. For the ITT, two-tailed Student's t-test were performed, # $p < 0.05$ gene effect $n = 6-7$.

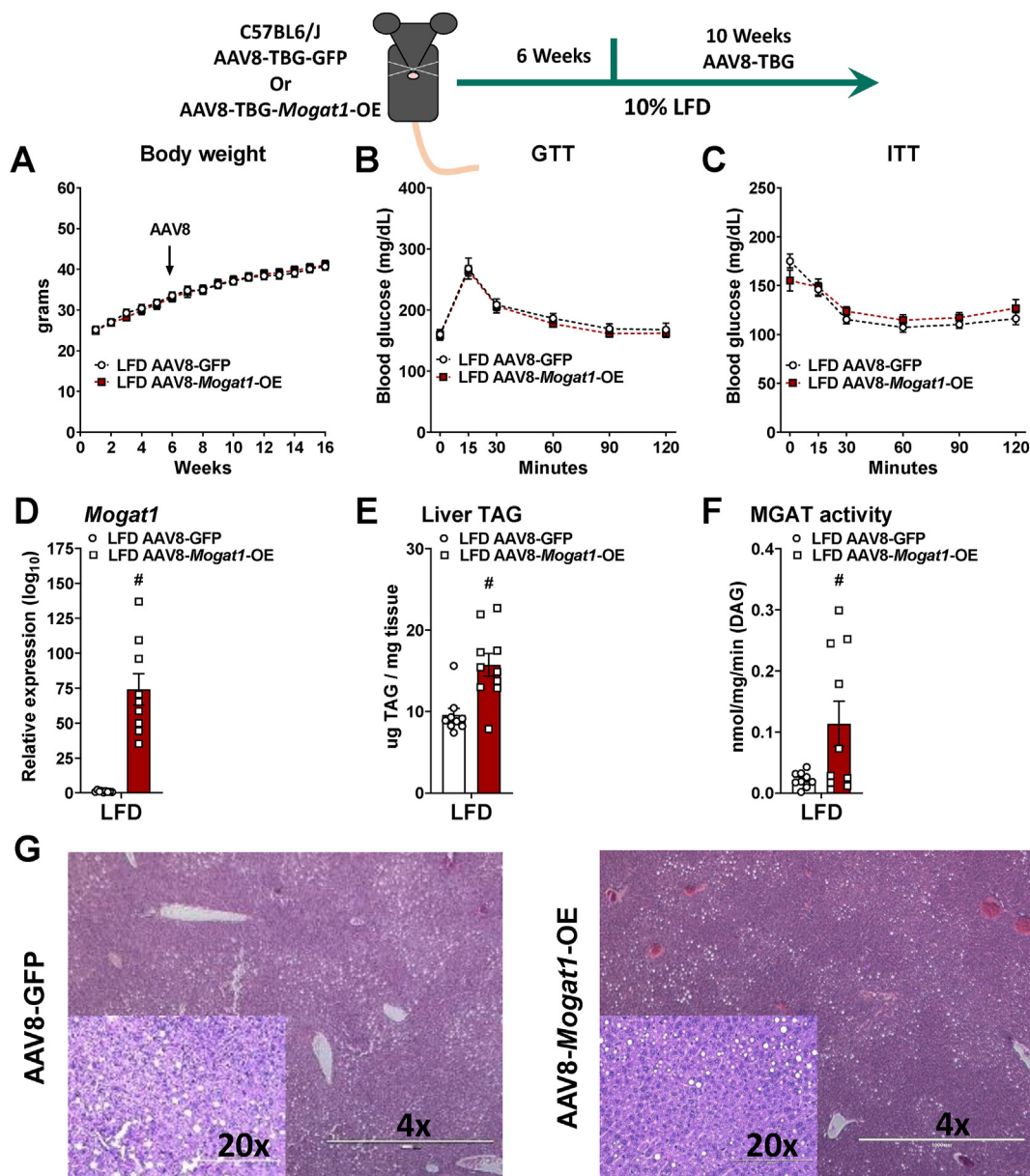


Figure 4: Hepatic *Mogat1* overexpression increases liver TAG and MGAT activity in mice fed an LFD. Male C57BL6/J mice were fed an LFD at 8 weeks of age. After 6 weeks of diet mice were injected (retro-orbital) with AAV8-TBG-GFP- or AAV8-TBG-*Mogat1* (2×10^{11} GC per mouse) and remained on the diet for an additional 10 weeks. Mice were fasted for 4 h prior to sacrifice and tissue collection. A: AAV8-*Mogat1*-OE did not affect body weight. B,C: *Mogat1* overexpression did not impair glucose or insulin tolerance. D: *Mogat1* gene expression was significantly increased in AAV8-*Mogat1*-OE treated mice. E,F: *Mogat1* overexpression increased both liver TAG and MGAT activity. G: H&E staining of liver sections reveals similar histology between groups. Data are expressed as means \pm S.E.M., and two-tailed Student's t-test were performed, [#] $p < 0.05$ gene effect, $n = 8-10$.

curve for WT and at 30 min post-injection for the MOKO mice (Figure 7A,B and Supplemental Figs. 4A and B). *Mogat1* ASO treatment lowered plasma insulin concentrations in WT mice and caused insulin to trend lower in MOKO mice treated with *Mogat1* ASO compared to control ASO (Figure 7C). *Mogat1* expression was nearly undetectable in the livers of MOKO mice and was reduced by *Mogat1* ASO only in WT mice (Figure 7D and Supplemental Fig. 4C).

Recently, McCabe et al. demonstrated that ASO targeting *TTC39B* non-specifically protects against diet-induced obesity and induces adipose tissue browning through activation of a type I interferon alpha/beta receptor 1 (IFNAR-1) in adipose tissue-derived macrophages even in *TTC39B* knockout mice [22]. Although we did not observe any effect on

body weight associated with use of the *Mogat1* ASO (Figure 6A), we found that expression of several key indicators of IFNAR-1 signaling (*Oas1*, *Iffit1*, and *Iffit2*) were significantly increased in MOKO mice treated with *Mogat1* ASOs (Figure 7E and Supplemental Fig. 4D). The *Mogat1* ASO also tended to increase the expression of these genes in WT mice, while *Iffar1* gene expression was unchanged (Figure 7E and Supplemental Fig. 4D).

3.7. IFNAR-1 blockade does not prevent improvements in glucose homeostasis in *Mogat1* ASO treated mice

To determine whether the increase in IFNAR-1 activation in response to *Mogat1* ASO treatment drives the improvements in glucose

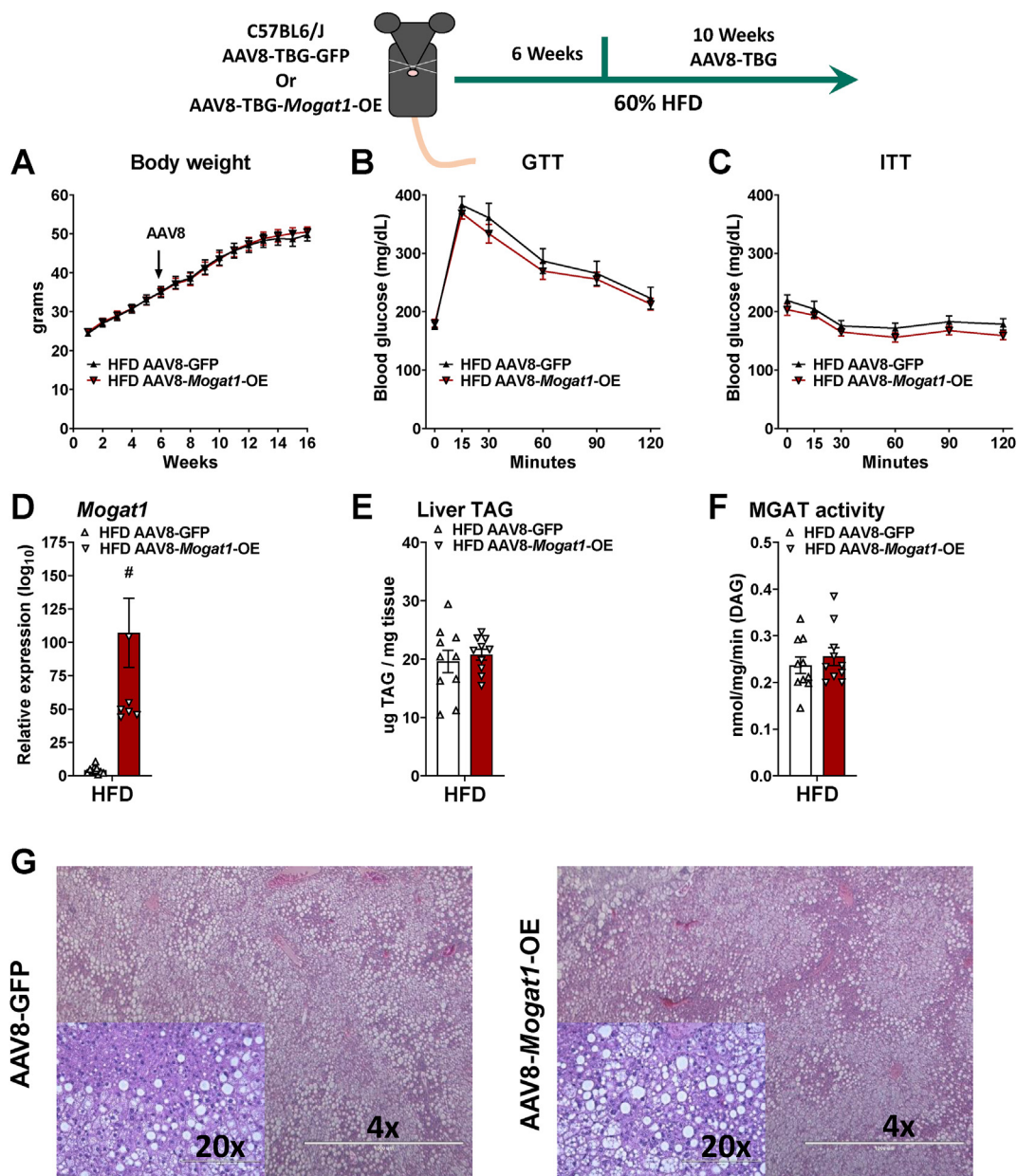


Figure 5: Hepatic *Mogat1* overexpression increases liver TAG and MGAT activity in mice fed the HFD. Male C57BL6/J mice were fed HFD at 8 weeks of age. After 6 weeks of diet, mice were injected (retro-orbital) with AAV8-TBG-GFP- or AAV8-TBG-*Mogat1* (2×10^{11} GC per mouse) and remained on the diet for an additional 10 weeks. Mice were fasted for 4 h prior to sacrifice and tissue collection. A: AAV8-*Mogat1*-OE did not affect body weight. B,C: *Mogat1* overexpression did not impair glucose or insulin tolerance. D: *Mogat1* gene expression was significantly increased in AAV8-*Mogat1*-OE treated mice. E,F: *Mogat1* overexpression did not affect liver TAG and MGAT activity. G: H&E staining of liver sections reveals similar histology between groups. Data are expressed as means \pm S.E.M. and two-tailed Student's t-test were performed, $\#p < 0.05$ gene effect, $n = 8-10$.

metabolism, we injected ASO treated mice with a IFNAR-1 neutralizing antibody or IgG control during an HFD challenge (Figure 8) [22,23]. We repeated the previous observation that this *Mogat1* ASO sequence improved glucose tolerance and lowered plasma insulin in HFD-fed mice (Figure 8A,B), but co-treatment with IFNAR-1 neutralizing antibody (INFAR1-Ab) did not block the improvements in glucose tolerance nor plasma insulin concentrations in *Mogat1* ASO-treated mice (Figure 8A-C). *Mogat1* ASO treatment suppressed liver *Mogat1* gene expression in IFNAR-1 neutralizing antibody-treated mice (Figure 8D). *Mogat1* ASO treatment did not significantly activate IFNAR-1-responsive genes in the livers of IgG-treated mice (Figure 8D) All of

these genes were lowered by use of the INFAR1-Ab (Figure 8D). *Mogat1* ASO treatment also suppressed *Mogat1* gene expression in epididymal white adipose tissue (WAT) (Figure 8E) but did not increase most INFAR-1 responsive genes in adipose tissue (Figure 8E). Lastly, *Mogat1* ASO treatment did not affect the expression of the WAT browning markers, *Ucp1*, *Ppargc1a*, or *Arb2*, which is in contrast to previous work (Figure 8F and ref [22]). In fact, *Arb2* was increased in mice treated with INFAR1-Ab regardless of which ASO mice received (Figure 8F).

Alternatively, our second ASO sequence targeting *Mogat1* had only modest effects on glucose tolerance and plasma insulin levels that

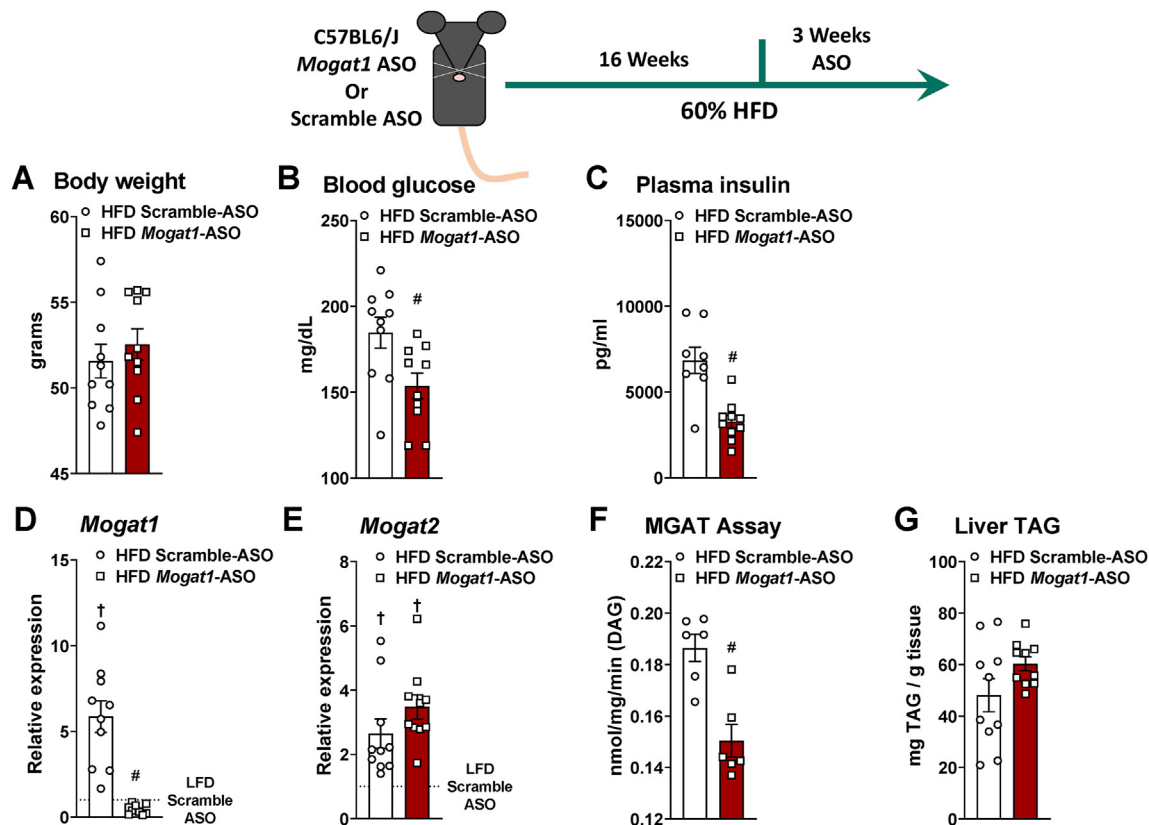


Figure 6: *Mogat1* antisense oligonucleotide (ASO) treatment improves insulin sensitivity in HFD fed mice. Male C57BL6/J mice were fed an HFD starting at 8 weeks of age. After 16 weeks of diet, mice were injected (intraperitoneally) twice weekly with ASOs targeted against *Mogat1* or scramble control (25 mg/kg) for 3 weeks. Mice were fasted for 4 h prior to sacrifice and tissue collection. A: Body weight was not affected by *Mogat1* ASO treatment. B,C: *Mogat1* ASO treatment reduced blood glucose and plasma insulin levels in mice fed an HFD. Gene expression was normalized to LFD-fed mice given scramble control. D: Hepatic *Mogat1* gene expression was increased in HFD-fed mice and significantly reduced by *Mogat1* ASO treatment. E: *Mogat2* gene expression was increased in HFD-fed mice. F,G: Hepatic MGAT activity was significantly reduced by *Mogat1* ASO treatment without affecting liver TAG. Data are expressed as means \pm S.E.M., and two-tailed Student's t-test or one-way ANOVA with Tukey's multiple comparison test were performed where appropriate, # $p < 0.05$ ASO effect, † $p < 0.05$ diet effect; $n = 5-10$.

were unaffected by the INFAR1-Ab treatment (Supplemental Figs. 5A–C). Similar reductions of *Mogat1* expression were observed in both liver and adipose tissue. However, the second sequence induced IFNAR-1 signaling in both liver and adipose tissue of IgG-treated mice, and these effects were suppressed by INFAR1-Ab treatment (Supplemental Figs. 5D and E). Finally, the second sequence induced epididymal *Ucp1* expression (Supplemental Fig. 5F). These data indicate that multiple *Mogat1* ASO treatments non-specifically improve glucose metabolism, and this effect is not mediated through the previously implicated mechanism of IFNAR-1 activation [22].

4. DISCUSSION

Increased intrahepatic lipid content is tightly and mechanistically linked to development of insulin resistance and systemic metabolic abnormalities. Previous work by our group and others using RNA interference approaches has demonstrated that knocking down expression of *Mogat1* in the livers of obese mice with hepatic steatosis dissociates liver fat from insulin resistance and improves glucose homeostasis [17,18,20,28]. In the present study, we knocked out *Mogat1* specifically in hepatocytes, both chronically and acutely, and also generated a global *Mogat1* knockout, but did not observe any improvements in glucose homeostasis or insulin sensitivity in diet-induced obese mice. Hepatic *Mogat1*

overexpression was sufficient to increase hepatic MGAT activity and TAG content, but only in LFD-fed mice, and did not result in insulin resistance or glucose intolerance. Although we reproduced our previous findings to demonstrate that multiple *Mogat1* ASOs improve glucose tolerance in obese mice, we also conclusively demonstrate that these ASOs still improve metabolic homeostasis in mice with global *Mogat1* deletion. Lastly, we confirm that these improvements were not due to increased activation of IFNAR-1 as recently reported for an ASO against TTC39B [22]. Collectively, these data suggest that *Mogat1* ASO treatment improves glucose homeostasis and insulin sensitivity independently of knocking down *Mogat1* expression and by mechanisms that remain to be elucidated.

The development of technologies for *in vivo* RNA interference through use of modified oligonucleotides has been a boon to hepatology and related disciplines. The ease of administration and liver-trophic nature of these designer oligonucleotides has allowed researchers to suppress the expression of a variety of genes in the liver and also led to clinically-approved approaches to treat metabolic disease [29,30]. Furthermore, in humans, unlike murine models, ASO treatment does not increase clinical indicators of liver and kidney injury [31] and next-generation ASO technology (GalNAc conjugation) has increased potency and reduced inflammation in the livers of mice, although their effects on off-target issues remains to be determined [21,32].

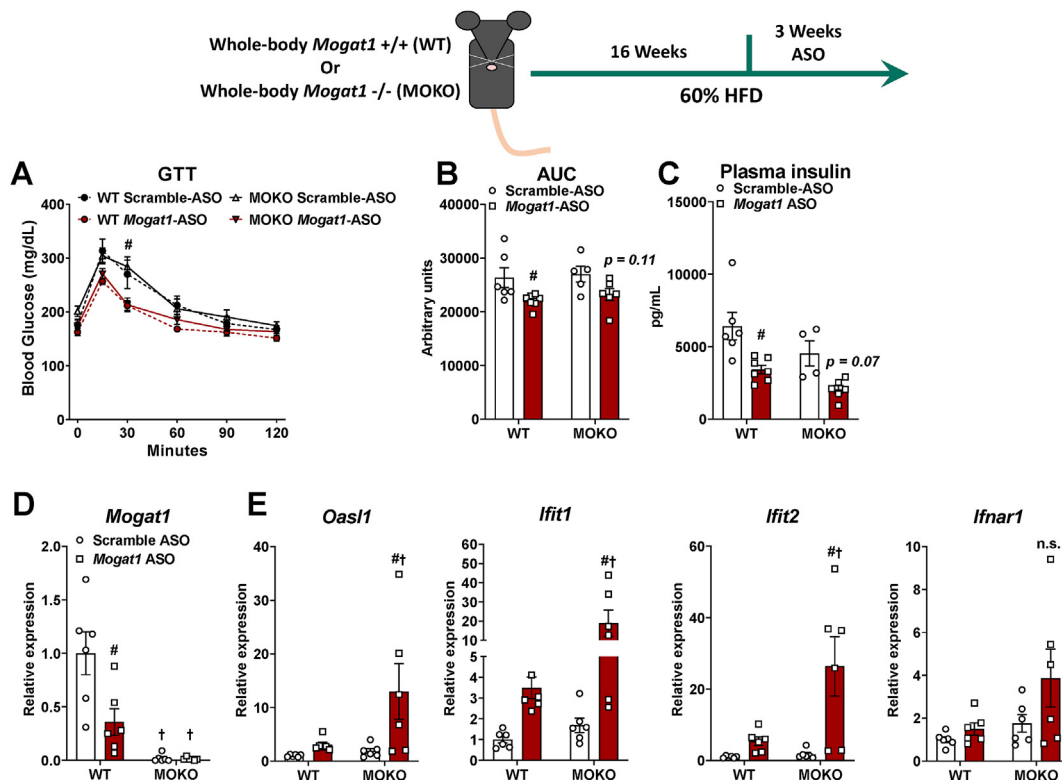


Figure 7: *Mogat1* ASO treatment improves glucose tolerance in whole-body *Mogat1* null mice on an HFD. Male wild-type (WT) and littermate *Mogat1* whole-body knockout (MOKO) mice were fed an HFD starting at 8 weeks of age. After 16 weeks of diet, mice were injected (intraperitoneal) twice weekly with ASOs targeted against *Mogat1* or scramble control (25 mg/kg) for 3 weeks. Mice were fasted for 4 h prior to sacrifice and tissue collection. A–C: *Mogat1* ASO treatment improves glucose tolerance and AUC independently of *Mogat1* expression and lowers plasma insulin in WT mice. D: *Mogat1* gene expression was reduced by ASO treatment and nearly absent in MOKO livers. E: Gene expression markers of interferon type-1 alpha/beta signaling are increased in *Mogat1* ASO treated MOKO mice on HFD. Data are expressed as means \pm S.E.M, and two-way ANOVA with Sidak's or Tukey's multiple comparison test were performed where appropriate # $p < 0.05$ from scramble ASO † $p < 0.05$ from WT controls; $n = 5-7$.

We were quite flummoxed when characterizing the phenotype of mice lacking *Mogat1* in liver by the inability to phenocopy our previously reported phenotypes obtained using ASOs [17,18,26] or work by other groups using adenoviral-driven expression of shRNA [20,28]. We considered a number of possibilities to explain this. It is likely that genetic deletion of *Mogat1* leads to compensatory changes in other enzymes that have MGAT activity, since ASO treatment leads to reduced MGAT activity in the liver [17], whereas MGAT knockout either acutely or chronically does not (Figures 1–3). Another possibility is that the *Mogat1* ASO was mediating its effects on a tissue other than liver. Brandon et al. recently reported that that liver-specific KO of protein kinase C ϵ (PKC ϵ) did not phenocopy previous ASO work conducted in rats and found instead that deletion of PKC ϵ in adipose tissue, which is often targeted by ASOs as well, produced an insulin-sensitive phenotype [33,34]. However, our studies with adipocyte-specific *Mogat1* KO mice (manuscript in preparation) or with the global MOKO mice did not reveal an insulin-sensitive phenotype. A caveat to this is that we did not assess the effects of a combined conditional *Mogat1* knockout in adipocytes and liver, two tissues primarily targeted by the *Mogat1* ASO, without deletion in other tissues that may have compensatory effects. This will require further consideration, but the observation that these ASOs have beneficial effects in MOKO mice suggests that the effects of the ASO is likely disconnected from the suppression of *Mogat1* expression. Taken together with previous work, these studies demonstrate the importance of using rigorous and complementary controls when employing ASOs to study intermediary metabolism and insulin sensitivity.

It is now clear that *Mogat1* ASOs elicit their effects even in the absence of *Mogat1* expression. In this work and in previous studies, we have used multiple ASO sequences targeting *Mogat1* with similar effects on glucose metabolism, and these effects do not appear to be due to silencing another gene from off-target interactions with RNA. The present results parallel another recent paper that showed that ASOs targeting TTC39B (T39) still elicited metabolic benefits in global T39 KO mice [22]. McCabe et al. [22] demonstrated in their model that ASO treatment activated an interferon signaling pathway as indicated by an induction of IFNAR-1 responsive genes (*Oasl1*, *Ifit1*, and *Ifit2*) that led to adipocyte browning and the mice to lose weight. Exactly how the interferon response is activated by ASO, how this occurs in the KO in the absence of target RNA, and why the scramble control ASO does not provoke the same response remains unclear. Although we did not observe weight loss in our studies, *Mogat1* ASO treatment in MOKO mice stimulated the expression of *Oasl1*, *Ifit1*, and *Ifit2* in liver. These responses were strikingly exaggerated in MOKO mice but in the WT mice, and we can only speculate that the lack of target RNA leads to higher non-hybridization dependent toxicity noted for many ASOs [35], while the scramble ASOs are designed to have minimal toxicities [21]. The activation of IFNAR-1 signaling may be consistent with our previous work demonstrating that *Mogat1* ASO exacerbates hepatic inflammation on a diet that induces nonalcoholic steatohepatitis, including components of interferon signaling [18,22]. While IFNAR-1 signaling activates a multitude of signaling pathways that could plausibly affect glucose metabolism and insulin sensitivity [36], we were unable to prevent the improvements in glucose metabolism

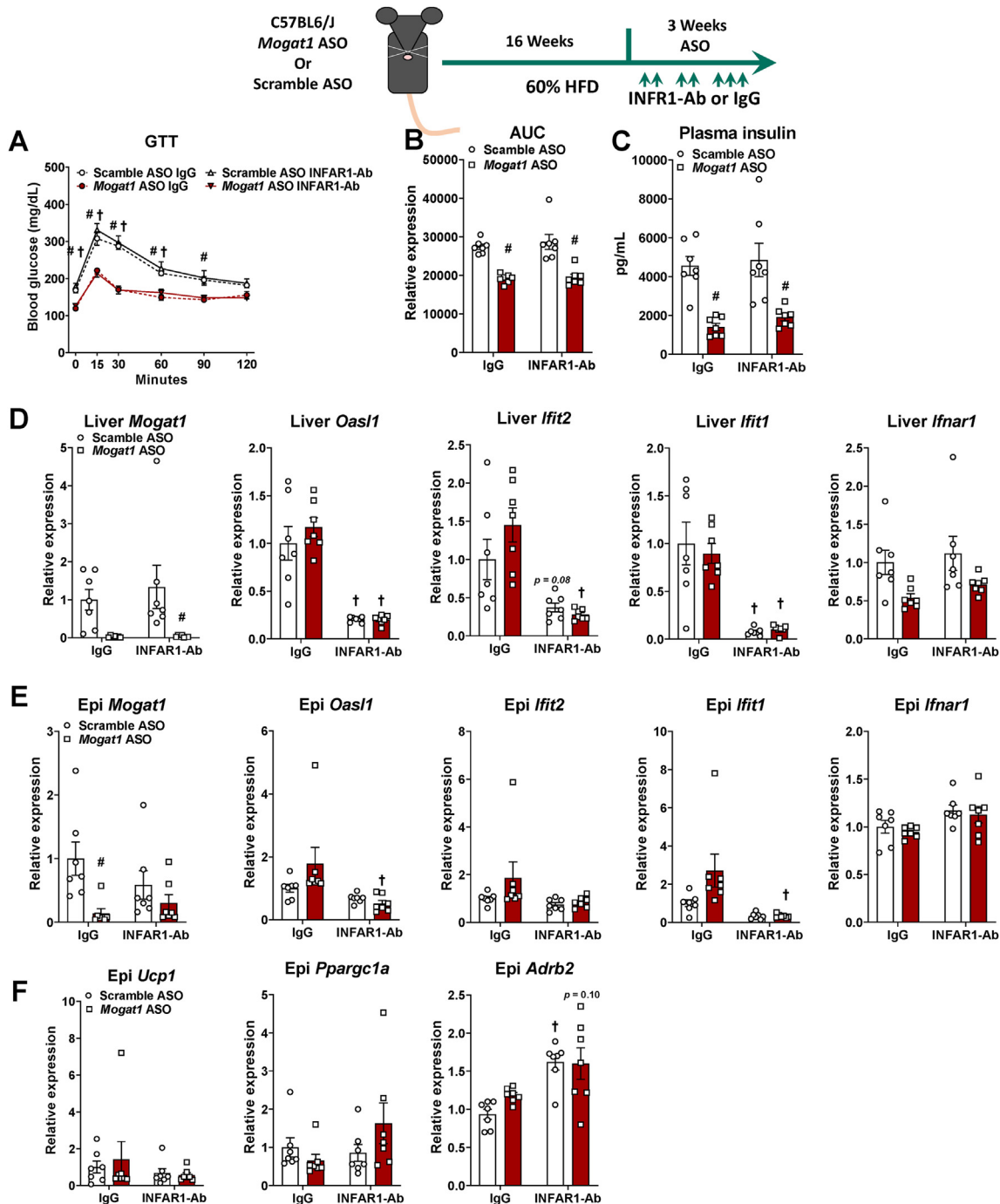


Figure 8: Type I interferon alpha/beta receptor 1 neutralizing antibody (INFAR1-Ab) prevents inflammation without affecting glucose tolerance. Male C57BL6/J mice were fed an HFD starting at 8 weeks of age. After 16 weeks of diet, mice were injected (intraperitoneal) twice weekly with ASOs targeted against *Mogat1* or scramble control (25 mg/kg) with an INFAR-1 neutralizing antibody (INFAR1-Ab) or IgG control (250 mg per mouse twice a week for weeks 1 and 2 and 500 mg per mouse 3 times for week 3). Mice were fasted for 4 h prior to sacrifice and tissue collection. A–C: *Mogat1* ASO treatment improves glucose tolerance and lowers plasma insulin despite INFAR1-Ab treatment. D: Liver *Mogat1* gene expression was reduced by *Mogat1* ASO treatment in the INFAR1-Ab treated mice and liver gene expression markers of interferon signaling are lowered by INFAR1-Ab treatment. E: Epididymal *Mogat1* gene expression was decreased by *Mogat1* ASO treatment. Epididymal gene expression markers of interferon signaling were not increased by *Mogat1* ASO treatment. F: Expression of adipose browning genes were not affected by *Mogat1* ASO treatment. Data are expressed as means \pm S.E.M and two-way ANOVA with Sidak's or Tukey's multiple comparison test where appropriate, # $p < 0.05$ from Scramble ASO † $p < 0.05$ from IgG controls; $n = 7$.

by blocking IFNAR-1 activation with an antibody. Thus, IFNAR-1 activation is not the mechanism for improved glucose and insulin tolerance in response to *Mogat1* ASO. However, we should note that the effects of the neutralizing antibody were not assessed in the MOKO mice,

which have a greater inflammatory response to *Mogat1* ASO. It is possible that the antibody could have an effect in MOKO mice, but given the complete lack of effect in WT mice, we feel that it is unlikely that it will. The mechanism by which *Mogat1* ASO elicits beneficial

metabolic effects, even in the absence of *Mogat1* RNA, will require further study.

Based on previous work with the *Mogat1* ASOs [17,18,26], we were surprised to find that genetic deletion of *Mogat1* in the liver did not affect hepatic MGAT activity. Our targeted allele deletes exon 4 of the *Mogat1* gene, which encodes the catalytic domain (HPHG), and we have previously shown that this effectively deletes all MGAT1 protein [15]. Moreover, the lack of effect on hepatic MGAT activity is consistent with previous work by another group with an independently-generated KO mouse showing that global *Mogat1* KO mice do not have deficits in hepatic MGAT activity [37]. Several acyltransferase enzymes exhibit MGAT activity, including MGAT2 and DGAT1, and the observation that genetic loss of MGAT1 in the liver did not affect MGAT activity could indicate that the other MGAT enzymes are the primary source of MGAT activity in the liver [10–13,15]. It is known that MGAT2 has a higher specific activity than MGAT1, and in many of the current studies, *Mogat2* was upregulated by HFD feeding. Our previous work has shown that adipocyte-specific *Mogat1* KO mice exhibit reduced adipose tissue MGAT activity [15], which may be consistent with the very low expression of *Mogat2* in adipose tissue. While we did not detect increased expression of the known MGAT enzymes in any of our genetic models [10–13], we cannot rule out post-transcriptional mechanisms, including post-translational modifications that enhance activity.

5. CONCLUSIONS

Here, we provide evidence that multiple *Mogat1* ASOs improve whole-body metabolism through *Mogat1*-independent effects. Liver-specific *Mogat1* ablation does not improve insulin resistance in HFD-fed mice, as observed with *Mogat1* ASO treatments [17,18]. Moreover, we show novel evidence that whole-body *Mogat1* deletion leads to insulin resistance in the context of diet-induced obesity. Finally, we provide preliminary evidence that *Mogat1* ASOs improve glucose intolerance even in global *Mogat1* KO mice. These findings also demonstrate that careful consideration should be given for using ASOs to target gene suppression, including use of genetic knockout models, in metabolic studies that could be affected by these off-target effects.

CONFLICT OF INTEREST

None declared.

ACKNOWLEDGMENTS

The authors would like to thank Dr. Kyle McCommis at St. Louis University for his insight into off-target effects of ASO treatments, Dr. Eric Yen at the University of Wisconsin for his advice on MGAT biology, Valerie Blanc for assistance with membrane preparations, and Daniel Ferguson for editing the manuscript during quarantine. We also thank the Washington University School of Medicine Nutrition and Obesity Research Center for continued support in research. Work in the authors' lab was supported by grants from the NIH (R56 DK111735) and the American Diabetes Association (1-17-IBS-109) to BNF and core laboratories of Washington University School of Medicine Diabetes Research Center (P30 DK020579), Digestive Diseases Research Cores Center, (P30 DK052574), and the Nutrition Obesity Research Center (P30 DK056341).

APPENDIX A. SUPPLEMENTARY DATA

Supplementary data to this article can be found online at <https://doi.org/10.1016/j.molmet.2021.101204>.

REFERENCES

- [1] Adams, L.A., Lymp, J.F., St Sauver, J., Sanderson, S.O., Lindor, K.D., Feldstein, A., et al., 2005. The natural history of nonalcoholic fatty liver disease: a population-based cohort study. *Gastroenterology* 129(1):113–121. <https://doi.org/10.1053/j.gastro.2005.04.014>.
- [2] Fabbrini, E., Sullivan, S., Klein, S., 2010. Obesity and nonalcoholic fatty liver disease: biochemical, metabolic, and clinical implications. *Hepatology* 51(2): 679–689. <https://doi.org/10.1002/hep.23280>.
- [3] Fabbrini, E., Yoshino, J., Yoshino, M., Magkos, F., Luecking, C.T., Samovski, D., et al., 2015. Metabolically normal obese people are protected from adverse effects following weight gain. *J Clin Invest* 125(2):787–795. <https://doi.org/10.1172/JCI78425>.
- [4] Lambert, J.E., Ramos-Roman, M.A., Browning, J.D., Parks, E.J., 2014. Increased de novo lipogenesis is a distinct characteristic of individuals with nonalcoholic fatty liver disease. *Gastroenterology* 146(3):726–735. <https://doi.org/10.1053/j.gastro.2013.11.049>.
- [5] Smith, G.I., Shankaran, M., Yoshino, M., Schweitzer, G.G., Chondronikola, M., Beals, J.W., et al., 2020. Insulin resistance drives hepatic de novo lipogenesis in nonalcoholic fatty liver disease. *J Clin Invest* 130(3):1453–1460. <https://doi.org/10.1172/JCI134165>.
- [6] Buzzetti, E., Pinzani, M., Tsochatzis, E.A., 2016. The multiple-hit pathogenesis of non-alcoholic fatty liver disease (NAFLD). *Metabolism* 65(8):1038–1048. <https://doi.org/10.1016/j.metabol.2015.12.012>.
- [7] Coleman, R.A., Lee, D.P., 2004. Enzymes of triacylglycerol synthesis and their regulation. *Prog Lipid Res* 43(2):134–176.
- [8] Chon, S.-H., Zhou, Y.X., Dixon, J.L., Storch, J., 2007. Intestinal monoacylglycerol metabolism: developmental and nutritional regulation of monoacylglycerol lipase and monoacylglycerol acyltransferase. *J Biol Chem* 282(46): 33346–33357. <https://doi.org/10.1074/jbc.M706994200>.
- [9] Han, G.-S., Wu, W.-I., Carman, G.M., 2006. The *Saccharomyces cerevisiae* Lipin homolog is a Mg²⁺-dependent phosphatidate phosphatase enzyme. *J Biol Chem* 281(14):9210–9218. <https://doi.org/10.1074/jbc.M600425200>.
- [10] Cao, J., Burn, P., Shi, Y., 2003. Properties of the mouse intestinal acyl-CoA: monoacylglycerol acyltransferase, MGAT2. *J Biol Chem* 278(28):25657–25663. <https://doi.org/10.1074/jbc.M302835200>.
- [11] Yen, C.-L.E., Stone, S.J., Cases, S., Zhou, P., Farese, R.V., 2002. Identification of a gene encoding MGAT1, a monoacylglycerol acyltransferase. *Proceedings of the National Academy of Sciences of the United States of America* 99(13): 8512–8517. <https://doi.org/10.1073/pnas.132274899>.
- [12] Yen, C.-L.E., Farese, R.V., 2003. MGAT2, a monoacylglycerol acyltransferase expressed in the small intestine. *J Biol Chem* 278(20):18532–18537. <https://doi.org/10.1074/jbc.M301633200>.
- [13] Cases, S., Smith, S.J., Zheng, Y.W., Myers, H.M., Lear, S.R., Sande, E., et al., 1998. Identification of a gene encoding an acyl CoA:diacylglycerol acyltransferase, a key enzyme in triacylglycerol synthesis. *Proceedings of the National Academy of Sciences of the United States of America* 95(22):13018–13023. <https://doi.org/10.1073/pnas.95.22.13018>.
- [14] Ho, S.-Y., Storch, J., 2001. Common mechanisms of monoacylglycerol and fatty acid uptake by human intestinal Caco-2 cells. *Am J Physiol Cell Physiol* 281(4):C1106–C1117. <https://doi.org/10.1152/ajpcell.2001.281.4.C1106>.
- [15] Liss, K.H.H., Lutkewitte, A.J., Pietka, T., Finck, B.N., Franczyk, M., Yoshino, J., et al., 2018. Metabolic importance of adipose tissue monoacylglycerol acyltransferase 1 in mice and humans. *J Lipid Res* M084947. <https://doi.org/10.1194/jlr.M084947>.
- [16] Hall, A.M., Kou, K., Chen, Z., Pietka, T.A., Kumar, M., Korenblat, K.M., et al., 2012. Evidence for regulated monoacylglycerol acyltransferase expression and activity in human liver. *J Lipid Res* 53(5):990–999. <https://doi.org/10.1194/jlr.P025536>.

- [17] Hall, A.M., Soufi, N., Chambers, K.T., Chen, Z., Schweitzer, G.G., McCommis, K.S., et al., 2014. Abrogating monoacylglycerol acyltransferase activity in liver improves glucose tolerance and hepatic insulin signaling in obese mice. *Diabetes* 63(7):2284–2296. <https://doi.org/10.2337/db13-1502>.
- [18] Soufi, N., Hall, A.M., Chen, Z., Yoshino, J., Collier, S.L., Mathews, J.C., et al., 2014. Inhibiting monoacylglycerol acyltransferase 1 ameliorates hepatic metabolic abnormalities but not inflammation and injury in mice. *J Biol Chem* 289(43):30177–30188. <https://doi.org/10.1074/jbc.M114.595850>.
- [19] Hayashi, Y., Suemitsu, E., Kajimoto, K., Sato, Y., Akhter, A., Sakurai, Y., et al., 2014. Hepatic monoacylglycerol O-acyltransferase 1 as a promising therapeutic target for steatosis, obesity, and type 2 diabetes. *Mol Ther Nucleic Acids* 3. <https://doi.org/10.1038/mtna.2014.4>.
- [20] Yu, J.H., Song, S.J., Kim, A., Choi, Y., Seok, J.W., Kim, H.J., et al., 2016. Suppression of PPAR γ -mediated monoacylglycerol O-acyltransferase 1 expression ameliorates alcoholic hepatic steatosis. *Scientific Reports* 6:29352. <https://doi.org/10.1038/srep29352>.
- [21] Geary, R., Norris, D., Bennett, F., Rosie, Y., 2015. Pharmacokinetics, bio-distribution and cell uptake of antisense oligonucleotides. *Adv Drug Deliv Rev* 87:46–51. <https://doi.org/10.1016/j.addr.2015.01.008>.
- [22] McCabe, K.M., Hsieh, J., Thomas, D.G., Molusky, M.M., Tascou, L., Feranil, J.B., et al., 2020. Antisense oligonucleotide treatment produces a type I interferon response that protects against diet-induced obesity. *Mol Metabol*. <https://doi.org/10.1016/j.molmet.2020.01.010>.
- [23] Wilson, E.B., Yamada, D.H., Elsaesser, H., Herskovitz, J., Deng, J., Cheng, G., et al., 2013. Blockade of chronic type I interferon signaling to control persistent LCMV infection. *Science* 340(6129):202–207. <https://doi.org/10.1126/science.1235208>.
- [24] Liss, K.H.H., Ek, S.E., Lutkewitte, A.J., Pietka, T.A., He, M., Skaria, P., et al., 2021. Monoacylglycerol acyltransferase 1 knockdown exacerbates hepatic ischemia-reperfusion injury in mice with hepatic steatosis. *Liver Transplantation*. <https://doi.org/10.1002/lt.25886> n/a(n/a).
- [25] McCommis, K.S., Chen, Z., Fu, X., McDonald, W.G., Colca, J.R., Kletzien, R.F., et al., 2015. Loss of mitochondrial pyruvate carrier 2 in the liver leads to defects in gluconeogenesis and compensation via pyruvate-alanine cycling. *Cell Metabolism* 22(4):682–694. <https://doi.org/10.1016/j.cmet.2015.07.028>.
- [26] Lutkewitte, A.J., McCommis, K.S., Schweitzer, G.G., Chambers, K.T., Graham, M.J., Wang, L., et al., 2019. Hepatic monoacylglycerol acyltransferase 1 is induced by prolonged food deprivation to modulate the hepatic fasting response. *J Lipid Res* M089722. <https://doi.org/10.1194/jlr.M089722>.
- [27] Cao, J., Cheng, L., Shi, Y., 2007. Catalytic properties of MGAT3, a putative triacylglycerol synthase. *J Lipid Res* 48(3):583–591. <https://doi.org/10.1194/jlr.M600331-JLR200>.
- [28] Lee, Y.J., Ko, E.H., Kim, J.E., Kim, E., Lee, H., Choi, H., et al., 2012. Nuclear receptor PPAR γ -regulated monoacylglycerol O-acyltransferase 1 (MGAT1) expression is responsible for the lipid accumulation in diet-induced hepatic steatosis. *Proceedings of the National Academy of Sciences of the United States of America* 109(34):13656–13661. <https://doi.org/10.1073/pnas.1203218109>.
- [29] Khvorova, A., Watts, J.K., 2017. The chemical evolution of oligonucleotide therapies of clinical utility. *Nature Biotechnology* 35(3):238–248. <https://doi.org/10.1038/nbt.3765>.
- [30] Rossor, A.M., Reilly, M.M., Sleight, J.N., 2018. Antisense oligonucleotides and other genetic therapies made simple. *Practical Neurology* 18(2):126–131. <https://doi.org/10.1136/practneurol-2017-001764>.
- [31] Crooke, S.T., Baker, B.F., Kwok, T.J., Cheng, W., Schulz, D.J., Xia, S., et al., 2016. Integrated safety assessment of 2'-O-methoxyethyl chimeric antisense oligonucleotides in NonHuman primates and healthy human volunteers. *Molecular Therapy: J American Society of Gene Therapy* 24(10):1771–1782. <https://doi.org/10.1038/mt.2016.136>.
- [32] Huang, Y., 2017. Preclinical and clinical advances of GalNAc-decorated nucleic acid therapeutics. *Molecular therapy. Nucleic Acids* 6:116–132. <https://doi.org/10.1016/j.omtn.2016.12.003>.
- [33] Samuel, V.T., Liu, Z.-X., Wang, A., Beddow, S.A., Geisler, J.G., Kahn, M., et al., 2007. Inhibition of protein kinase C ϵ prevents hepatic insulin resistance in nonalcoholic fatty liver disease. *J Clin Invest* 117(3):739–745. <https://doi.org/10.1172/JCI30400>.
- [34] Brandon, A.E., Liao, B.M., Diakanastasis, B., Parker, B.L., Raddatz, K., McManus, S.A., et al., 2019. Protein kinase C epsilon deletion in adipose tissue, but not in liver, improves glucose tolerance. *Cell Metabolism* 29(1):183–191. <https://doi.org/10.1016/j.cmet.2018.09.013> e7.
- [35] Frazier, K.S., 2015. Antisense oligonucleotide therapies: the promise and the challenges from a toxicologic pathologist's perspective. *Toxicologic Pathology* 43(1):78–89. <https://doi.org/10.1177/0192623314551840>.
- [36] Dodington, D.W., Desai, H.R., Woo, M., 2018. JAK/STAT — emerging players in metabolism. *Trends Endocrinol Metabol* 29(1):55–65. <https://doi.org/10.1016/j.tem.2017.11.001>.
- [37] Agarwal, A.K., Tunison, K., Dalal, J.S., Yen, C.-L.E., Farese, R.V., Horton, J.D., et al., 2016. Mogat1 deletion does not ameliorate hepatic steatosis in lipodystrophic (Agpat2 $^{-/-}$) or obese (ob/ob) mice. *J Lipid Res* 57(4):616–630. <https://doi.org/10.1194/jlr.M065896>.